Inclusive ω photoproduction from nuclei and ω in the nuclear medium

M. Kaskulov[1,a], E. Hernandez[2,b], and E. Oset[1,c]

[1] Departamento de Física Teórica and IFIC, Centro Mixto Universidad de Valencia-CSIC, Institutos de Investigación de Paterna, Aptd. 22085, 46071 Valencia, Spain
[2] Grupo de Física Nuclear, Departamento de Fisica Fundamental e IUFFyM, Facultad de Ciencias, Universidad de Salamanca, Plaza de la Merced s/n, E-37008 Salamanca, Spain

Abstract. With the aim of extracting information on the shift of the ω mass in the nuclear medium we analyze data obtained at ELSA from where claims for evidence of a mass shift of the ω have been made. We develop a Monte Carlo simulation code which takes into account the possible reactions in the experimental set-up of $(\gamma A \to \pi^0 \gamma X)$ in the vicinity of the ω production region with subsequent $\omega \to \pi^0 \gamma$ decay. We compare our results with experiment for the distribution of $\pi^0 \gamma$ invariant masses and conclude that the distribution is compatible with an enlarged ω width of about 90 MeV at nuclear-matter density and no shift in the mass. This change in the width would be compatible with the preliminary results obtained from the transparency ratio in the A-dependence of ω production. The discrepancy of the present conclusions with former claims of an evidence for a shift of the ω mass stems from a different choice of background which is discussed in the paper.

PACS. 24.80.+y Nuclear tests of fundamental interactions and symmetries – 25.20.-x Photonuclear reactions – 11.30.Rd Chiral symmetries – 13.60.Le Meson production

1 Introduction

The interaction of mesons with nuclei has captured the attention of the hadron community and much work has been done on the topic [1]. In particular the behavior of vector mesons in nuclei has been thoroughly studied, stimulated by the ansatz of a universal scaling of the vector meson masses in nuclei suggested in [2] and the study of QCD sum rules in nuclei [3], although earlier studies within the Nambu-Jona-Lasinio model produced no dropping of the vector meson masses [4]. Most of the efforts have been devoted to the change of the ρ properties in the medium, but the properties of the ω-meson have also received much attention and many theoretical efforts have been devoted to obtain the changes of the mass and width in the medium [5–22]. The values obtained for the self-energy of the ω in nuclei split nearly equally into attraction and repulsion and range from an attraction of the order of 100–200 MeV [8,10] to no changes in the mass [20] to a net repulsion of the order of 50 MeV [16].

[a] e-mail: Murat.Kaskulov@theo.physik.uni-giessen.de
[b] e-mail: gajatee@usal.es
[c] e-mail: oset@ific.uv.es

While most of the experimental work is conducted in heavy-ion reactions, it has been argued in [23] that reactions involving the interaction of elementary particles with nuclei can be equally good to show medium effects of particles, with the advantage of being easier to analyze. In this sense, a variety of experiments have been done with pA collisions in nuclei at KEK [24–26] and photonuclear collisions at Jefferson Lab [27] by looking at dilepton spectra.

A different approach has been followed by the CBELSA/TAPS Collaboration by looking at the $\gamma\pi^0$ coming from the ω decay. In this line a recent work [28] claims evidence for a decrease of the ω mass in the medium of the order of 100 MeV from the study of the modification of the mass spectra in ω photoproduction.

In the present work we perform a reanalysis of the data of [28]. We develop a Monte Carlo simulation code which takes into account the possible reactions in the experimental set-up of $(\gamma A \to \pi^0 \gamma X)$ in the vicinity of the ω production region with subsequent $\omega \to \pi^0 \gamma$ decay. Especial emphasis is done in the final-state interaction of the particles produced in order to properly reconstruct the invariant mass of the $\pi^0 \gamma$ subsystem. We first look at the A-dependence of the ω production (transparency ratio)

from where, in base to preliminary data, we induce an approximate width of the ω in the nuclear medium. Next, we compare our results with experiment for the distribution of $\pi^0\gamma$ invariant masses and conclude that the distribution is compatible with an enlarged ω width of about 90 MeV at nuclear-matter density and no shift in the mass. The discrepancy of the present conclusions with former claims of an evidence for a shift of the ω mass stems from a different choice of background. We show that the former claims were based on an assumption of background which eliminates strength at high ω masses, while the choice of background scaled from the elementary reaction automatically leads to strength at high ω masses, as well as in lower masses, which can be explained by means of an increased ω width, that is also compatible with the preliminary results obtained from the transparency ratio.

The paper proceeds as follows: In sect. 2 we outline the results of the microscopic calculations which serves here as input for our computer simulation. In sects. 3 and 4 we provide the details of the Monte Carlo simulation method. The results are presented in sects. 5, 6 and 7. The conclusions are given in sect. 8.

2 Preliminaries

The inclusive reactions like the one studied here, $A(\gamma, \omega \to \pi^0\gamma)X$, require minimum knowledge of nuclear structure, since one is not looking at any particular final nuclear state but integrating over all of them. Assuming further that the elementary production amplitude on a single nucleon has been fixed, in a first step, the nuclear cross-section can be obtained by summing over the occupied nuclear states in the Fermi sea and by introducing the standard nuclear effects like the Fermi motion of the initial nucleons and the Pauli blocking (for the $\gamma N \to \omega N$) of the outgoing ones.

In the present work we go beyond this scheme and consider also the final-state interaction (FSI) of the ω-mesons and its decay products in finite nuclei. The method used here will combine a phenomenological calculation of the intrinsic probabilities for different nuclear reaction, like the quasielastic and absorption channels, as a function of the nuclear-matter density, followed by a computer Monte Carlo (MC) simulation procedure in order to trace the fate of the ω-mesons and its decay products in the nuclear medium. Since our calculations represent complete event simulations it will be possible to account for the actual experimental acceptance effects. In the following we shall carry out the computer MC simulation taking into account the geometrical and kinematical acceptance conditions of the Crystal Barrel/TAPS experiment at ELSA.

We consider the photonuclear reaction $A(\gamma, \omega \to \pi^0\gamma)X$ in two steps —production of the ω-mesons and propagation of the final states. In the laboratory, where the nucleus with the mass number A is at rest, the nuclear total cross-section of the inclusive reaction $A(\gamma, \omega)X$ including the effects of Fermi motion and Pauli blocking is

given by

$$
\sigma_{\gamma A \to \omega X} =
$$
$$
\int_A \frac{\mathrm{d}^3\vec{r}}{2\pi^2} \int \frac{\mathrm{d}^3\vec{p}_N}{(2\pi)^3} \int \mathrm{d}\widetilde{m}_\omega^2 \frac{S_\omega(m_\omega, \widetilde{m}_\omega, \rho_A(r))M_N^2}{|\vec{p}_\gamma + \vec{p}_N|[(p_\gamma + p_N)^2 - M_N^2]}
$$
$$
\times \int \mathrm{d}E_\omega \int_0^{2\pi} \mathrm{d}\varphi_\omega \left(\overline{\sum_{\mathrm{in}}}\sum_{\mathrm{out}} T^\dagger T\right)_{\gamma N \to \omega N} \Theta(1 - B^2)
$$
$$
\times \Theta(k_F(r) - |\vec{p}_N|)\,\Theta(E_\gamma + E_N - E_\omega - E_F(r))
$$
$$
\times \Omega_\omega(\vec{r}, \rho(r), \vec{p}_\omega, \widetilde{m}_\omega). \tag{1}
$$

Here Θ denotes the step function and B stands for the cosinus of the angle between $\vec{p}_\gamma + \vec{p}_N$ and $\vec{p}_\omega$

$$
B \equiv \cos\vartheta_\omega = \frac{1}{2\,|\vec{p}_\omega||\vec{p}_\gamma + \vec{p}_N|} \tag{2}
$$
$$
\times \left[(\vec{p}_\gamma + \vec{p}_N)^2 + \vec{p}_\omega^2 + M_N^2 - (E_\gamma + E_N - E_\omega)^2\right]
$$

with obvious notations for the momenta and energies of the particles $E_\gamma = |\vec{p}_\gamma|$, $E_\omega = \sqrt{\vec{p}_\omega^2 + \widetilde{m}_\omega^2}$ and $E_N = \sqrt{\vec{p}_N^2 + M_N^2}$. Also in eq. (1) $E_F(r) = \sqrt{k_F^2(r) + M_N^2}$ is the local Fermi energy and the Fermi momentum k_F is related to the local density $\rho_A(r)$ of the nucleus by

$$
\rho_A(r) = 4 \int \frac{\mathrm{d}^3\vec{p}_N}{(2\pi)^3}\Theta(k_F(r) - |\vec{p}_N|) = \frac{2\,k_F^3(r)}{3\pi^2}. \tag{3}
$$

The photoproduction amplitude entering eq. (1) is that from the elementary reaction $N(\gamma, \omega)N$ properly summed and averaged over the final and initial polarizations, respectively. It is given by

$$
\overline{\sum_{\mathrm{in}}}\sum_{\mathrm{out}} T^\dagger T = \frac{16\pi s E_\gamma^{*2}}{M_N^2} \frac{\mathrm{d}\sigma_{\gamma N \to \omega N}}{\mathrm{d}t}, \tag{4}
$$

where $\mathrm{d}\sigma_{\gamma N \to \omega N}/\mathrm{d}t$ is an invariant differential cross-section with $s = (p_\gamma + p_N)^2$, $E_\gamma^* = \frac{s - M_N^2}{2\sqrt{s}}$ and $t = (p_\omega^{lab} - p_\gamma)^2$ where p_ω^{lab} is the four-momentum of the ω in the laboratory frame. In eq. (1) the momentum $\vec{p}_\omega = (|\vec{p}_\omega|, \vartheta_\omega, \varphi_\omega)$ of the ω is defined with respect to $\vec{p}_\gamma + \vec{p}_N = (|\vec{p}_\gamma + \vec{p}_N|, \vartheta', \varphi')$. Making use of ordinary rotation matrices $\mathcal{R}_{\varphi'}$ and $\mathcal{R}_{\vartheta'}$ one can transform $\vec{p}_\omega$ to the laboratory system where it takes the form

$$
\vec{p}_\omega^{lab} = \mathcal{R}_{\varphi'} \otimes \mathcal{R}_{\vartheta'} \otimes \vec{p}_\omega \tag{5}
$$

with

$$
\mathcal{R}_{\varphi'} = \begin{pmatrix} \cos\varphi' & -\sin\varphi' & 0 \\ \sin\varphi' & \cos\varphi' & 0 \\ 0 & 0 & 1 \end{pmatrix}, \quad \mathcal{R}_{\vartheta'} = \begin{pmatrix} \cos\vartheta' & 0 & \sin\vartheta' \\ 0 & 1 & 0 \\ -\sin\vartheta' & 0 & \cos\vartheta' \end{pmatrix}. \tag{6}
$$

In ref. [29] $\mathrm{d}\sigma_{\gamma p \to \omega p}/\mathrm{d}t$ of the reaction (γ, ω) on the hydrogen target followed by the $\omega \to \pi\pi\pi$ decay has been measured for incident photon energies from the reaction threshold $E_\gamma^{th} = m_\omega + m_\omega^2/2M_p \simeq 1.1$ GeV up to 2.6 GeV.
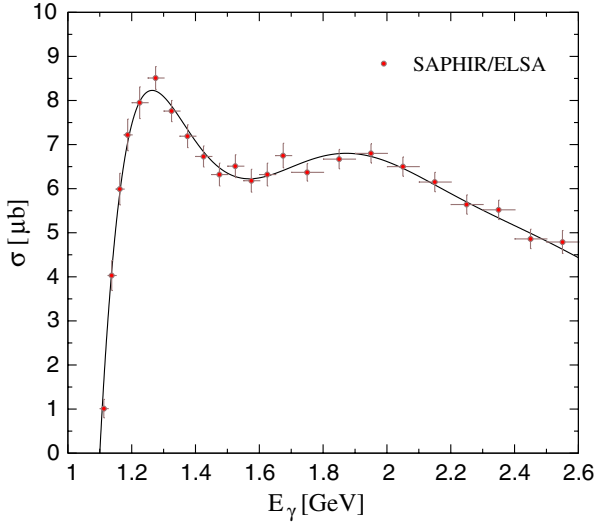
Fig. 1. Total cross-section of the reaction $p(\gamma, \omega)p$ as a function of the photon energy E_γ. The experimental data are from ref. [29]. The solid curve is the fit to data.

In the present work the data of ref. [29] are conveniently parameterized and properly implemented in the MC code. The fit to the total cross-section is presented in fig. 1 where the experimental data from ref. [29] are also shown. In the following, the cross-section on the neutron will be taken to be the same as on a proton.

The ω-mesons are produced according to their spectral function S_ω at a local density $\rho(r)$

$$S_\omega(m_\omega, \widetilde{m}_\omega, \rho) = -\frac{1}{\pi} \frac{\mathrm{Im}\,\Pi_\omega(\rho)}{\left(\widetilde{m}_\omega^2 - m_\omega^2 - \mathrm{Re}\,\Pi_\omega(\rho)\right)^2 + \left(\mathrm{Im}\,\Pi_\omega(\rho)\right)^2}, \quad (7)$$

where Π_ω is the in-medium self-energy of the ω with nominal mass $m_\omega = 782\,\mathrm{MeV}$. The width of the ω in the nuclear medium is related to the self-energy by $\Gamma_\omega(\rho, \widetilde{m}_\omega) = -\mathrm{Im}\,\Pi_\omega(\rho, \widetilde{m}_\omega)/E_\omega$. It includes the free width $\Gamma_{free} = 8.49\,\mathrm{MeV}$ and an in-medium part $\Gamma_{coll}(\rho)$ which accounts for the collisional broadening of the ω due to the quasielastic and absorption channels to be specified below. In eq. (7) $\mathrm{Re}\,\Pi_\omega = 2E_\omega \mathrm{Re}\,V_{opt}(\rho)$, where $V_{opt}(\rho)$ is the ω nucleus optical potential accounts for a possible shift of the ω mass in the medium and we shall make some considerations about it later on.

In eq. (1) the distortion factor Ω_ω describes the propagation and decay of the ω-mesons inside and outside the nucleus as well as the FSI of its decay products —in our case $\pi^0\gamma$— in the nuclear medium. It is the subject of the present MC simulation.

In the following we shall also consider the situation when the energy of the incident photon beam is not fixed but constrained in some energy interval $E_\gamma^{\min} < E_\gamma < E_\gamma^{\max}$. This condition is implemented by folding the cross-section of eq. (1) with the photon flux profile

$$\int_{E_\gamma^{\min}}^{E_\gamma^{\max}} \mathrm{d}E_\gamma\, W_\gamma(E_\gamma)\, \sigma_{\gamma A \to \omega X}. \quad (8)$$

At the ELSA facility, the photon beam is produced via the electron bremsstrahlung and therefore one creates the photon flux according to the unnormalized spectra

$$W_\gamma(E_\gamma) = \frac{1}{N_\gamma} \frac{\mathrm{d}N_\gamma}{\mathrm{d}E_\gamma} \propto \frac{1}{E_\gamma}. \quad (9)$$

3 The Monte Carlo simulation procedure

The computer MC simulation proceeds in close analogy to the actual experiment. At first, the multiple integral in eq. (1) is carried out using the MC integration method. This procedure provides a random point $\vec{r}$ inside the nucleus where the photon collides with the nucleon, also randomly generated from the Fermi sea with $|\vec{p}_N| \leq k_F(\vec{r})$, see the factor $\Theta(k_F(\vec{r}) - |\vec{p}_N|)$ in eq. (1). For the sample event in the MC integral the mass $\widetilde{m}_\omega$ of the ω respects the spectral function S_ω at local density $\rho(r)$, see eq. (7). Inside the nucleus the ω-mesons moving with the three-momentum $\vec{p}_\omega^{lab}$ necessarily interact with the nucleons in their way out of the nucleus. In the MC simulation the ω-mesons are allowed to propagate a distance $\delta\vec{L} = \frac{\vec{p}_\omega^{lab}}{|\vec{p}_\omega^{lab}|}\delta L$ and at each step, $\delta L \simeq 0.1\,\mathrm{fm}$, the reaction probabilities for different channels like the decay of the ω into $\pi^0\gamma$ and $\pi\pi\pi$ final states, quasielastic scattering and in-medium absorption are properly calculated. The value of δL is chosen such that smaller values do not change the results within the statistical errors of our MC procedure, which are much smaller than the experimental errors.

The conventional decay channels are $\omega \to \pi\pi\pi$ and $\omega \to \pi^0\gamma$ and the corresponding reaction probabilities per unit length are given by

$$\frac{\delta P_{\omega \to \pi\pi\pi}}{\delta L} = \frac{1}{\gamma v} \Gamma_{\omega \to \pi\pi\pi} = \frac{m_\omega}{|\vec{p}_\omega|} \Gamma_{\omega \to \pi\pi\pi}, \quad (10)$$

$$\frac{\delta P_{\omega \to \pi\gamma}}{\delta L} = \frac{1}{\gamma v} \Gamma_{\omega \to \pi\gamma} = \frac{m_\omega}{|\vec{p}_\omega|} \Gamma_{\omega \to \pi\gamma}, \quad (11)$$

where $v = |\vec{p}_\omega|/E_\omega$ is the ω velocity and the Lorentz contraction factor $\gamma = E_\omega/m_\omega$ relates the width of the ω in the rest frame, Γ_ω, to that in the moving frame Γ_ω^*. The partial decay width of the ω into $\pi\pi\pi$ and $\pi^0\gamma$ decay channels are $\Gamma_{\omega \to \pi\pi\pi} \simeq 7.56\,\mathrm{MeV}$ and $\Gamma_{\omega \to \pi\gamma} \simeq 0.76\,\mathrm{MeV}$, respectively [30].

At given local density $\rho(r)$, the probability per unit length for the quasielastic collision of the ω is given by

$$\frac{\delta P_{CB}}{\delta L} = \sigma_{\omega N \to \omega N}\,\rho(r), \quad (12)$$

where $\sigma_{\omega N \to \omega N}$ stands for the elastic $\omega N \to \omega N$ cross-section. In the present work we employ the parameterization of the $\sigma_{\omega N \to \omega N}$ used in refs. [13,21]. For the sample quasielastic event the angular distributions (we assume s-wave) are generated in the c.m. frame of the ω and a random nucleon in the Fermi sea. Then, a Lorentz boost back to the laboratory is done in order to obtain the energy and momentum of the scattered ω and outgoing nucleon after the quasielastic step. Since the outgoing nucleon moving

with the three-momentum $|\vec{p}'_N|$ is subject to Pauli blocking, we require that the quasielastic scattering fulfills the condition $|\vec{p}'_N| > k_F(r)$. These quasielastic steps barely modify the ω production rate and the ω invariant mass distribution since they respect the original direction of the ω as an average and, although they modify a bit the ω energy, they do not modify its invariant mass to be studied in sect. 7.

The in-medium $\omega N \to \omega N$ elastic scattering does not lead to a loss of flux and does not change the total nuclear cross-section. It affects the ω energy and momentum distributions only increasing the energy loss of the ω in MC steps. The loss of the ω flux is related to the absorptive part of the ω-nucleus optical potential. In nuclear matter, the ω-wave propagating through will acquire the phase $\sim \exp(-iV_{opt}^{abs}t)$ which enforce the ω to be removed from the elastic flux at the rate

$$\frac{1}{N_\omega}\frac{\mathrm{d}N_\omega}{\mathrm{d}t} \equiv \frac{\delta P_{abs}}{\mathrm{d}t} = \Gamma_{abs} = -2\,\mathrm{Im}\,V_{opt}^{abs}, \qquad (13)$$

where V_{opt}^{abs} is the part of the $\mathrm{Im}\,V_{opt}$ related to the ωN inelastic cross-section σ_{in} and other many-body absorption mechanisms.

The reaction probability for the ω-meson to be absorbed inside the nucleus after the propagation of the length interval δL or undergo inelastic collision is given by

$$\frac{\delta P_{abs}}{\delta L} = \frac{1}{v}\Gamma_{abs}. \qquad (14)$$

As a first estimate, we use the following parameterization for the width:

$$\Gamma_{abs} = \Gamma_0 \frac{\rho(r)}{\rho_0}, \qquad (15)$$

where $\rho_0 = 0.16\,\mathrm{fm}^{-3}$ is the normal nuclear-matter density. The parameterization is adequate for the inelastic processes and only approximate for the absorption processes which would be better represented by a ρ^2 functional. It is thus implicit that the ρ functional for the absorption provides the correct absorption width for the average density felt by the process.

Since we are interested in $\pi^0\gamma$ events, the absorption channels and decay $\omega \to \pi\pi\pi$ remove the ω-mesons from the initial flux. The $\pi^0\gamma$ events may come from both the ω decaying inside and outside the nucleus. Only $\pi^0\gamma$ events from $\omega \to \pi^0\gamma$ decays inside the nucleus carry information on the ω in-medium properties. If the resonance leaves the nucleus, its spectral function must coincide with the free distribution, $\mathrm{Im}\,\Pi_\omega = -\widetilde{m}_\omega \Gamma_\omega^{free}$, because the collisional part of the width is zero in this case. When the ω decays into the $\pi^0\gamma$ pair at the point $\vec{r}'$ inside the nucleus its mass distribution is generated according to the in-medium spectral function at the local density $\rho(r')$. For a given mass $\widetilde{m}_\omega$ the ω-mesons are allowed to decay isotropically in the c.m. system into the $\pi^0\gamma$ channel. The direction of the π^0 (therefore γ) is then chosen randomly and an appropriate Lorentz transformation is done in order to generate the corresponding $\pi^0\gamma$ distributions in the laboratory frame. The ω-mesons are reconstructed using the energy and momentum of the $\pi^0\gamma$ pair in the laboratory.

4 Propagation of pions in nuclei

The reconstruction of the genuine $\omega \to \pi^0\gamma$ mode is affected by the FSI of the π^0 in the nucleus which distorts the $\pi^0\gamma$ spectra. In this case, if the π^0 events come from the interior of the nucleus we trace the fate of the neutral pions starting from the decay point of the ω-meson. In their way out of the nucleus pions can experience the quasielastic scattering or can be absorbed. The intrinsic probabilities for these reactions as a function of the nuclear-matter density are calculated using the phenomenological models of refs. [31–33], which also include higher-order quasielastic cuts and the two-body and three-body absorption mechanisms. Since the FSI of the γ quanta are rather weak, they are allowed to escape the nucleus without distortion. In this section we briefly summarize the approach used for the description of the pion propagation in nuclei.

We consider different energy regions where the pions appear, according to their kinetic energy T_π. In the $\Delta(1232)$ region we use the microscopic Δh model for the pion nuclear interaction [31,32]. The formulae for the probabilities per unit length that a pion undergoes quasielastic scattering P_{QE} (for $T_\pi \leq 390\,\mathrm{MeV}$) and that the pion is absorbed P_A (for $T_\pi \leq 315\,\mathrm{MeV}$) are adopted from ref. [34]. The latter includes higher-order quasielastic cuts and also the parts corresponding to the two-body and three-body absorption cuts.

Beyond the $\Delta(1232)$-isobar region, we rely upon elementary π-nucleon cross-sections, which provide the probability per unit length for a certain reaction to happen. For instance, in that region the probability that a pion undergoes a quasielastic scattering P_Q is given by

$$\frac{\delta P_{QE}}{\delta L} = \bar{\sigma}_{QE}\rho(r), \qquad (16)$$

where $\bar{\sigma}_{QE}$ is an average of the $\pi^0 p \to \pi^0 p$ and $\pi^0 n \to \pi^0 n$ cross-sections. It can be determined using the isospin formalism in terms of the experimentally accessible cross-sections taken from ref. [35]

$$\begin{aligned}\bar{\sigma}_{QE} &\equiv \frac{1}{2}(\sigma_{\pi^0 p \to \pi^0 p} + \sigma_{\pi^0 n \to \pi^0 n})\\ &= \frac{1}{2}(\sigma_{\pi^+ p \to \pi^+ p} + \sigma_{\pi^- p \to \pi^- p} - \sigma_{\pi^- p \to \pi^0 n}). \end{aligned} \qquad (17)$$

For the given quasielastic event the angular distributions are generated in the c.m. frame of the pion and a random nucleon in the Fermi sea. Then a Lorentz boost back to the laboratory is done in order to obtain the energy and momentum of the pion and outgoing nucleon after the quasielastic step. Since the outgoing nucleon moving with the three-momentum $|\vec{p}'_N|$ is subject to Pauli blocking, we require that the quasielastic scattering fulfills the condition $|\vec{p}'_N| > k_F(r)$.

Making use of the isospin amplitudes we get for the charge exchange reaction the following cross-section:

$$\bar{\sigma}_{CX} \equiv \frac{1}{2}(\sigma_{\pi^0 n \to \pi^- p} + \sigma_{\pi^0 p \to \pi^+ n}) = \sigma_{\pi^- p \to \pi^0 n}. \qquad (18)$$
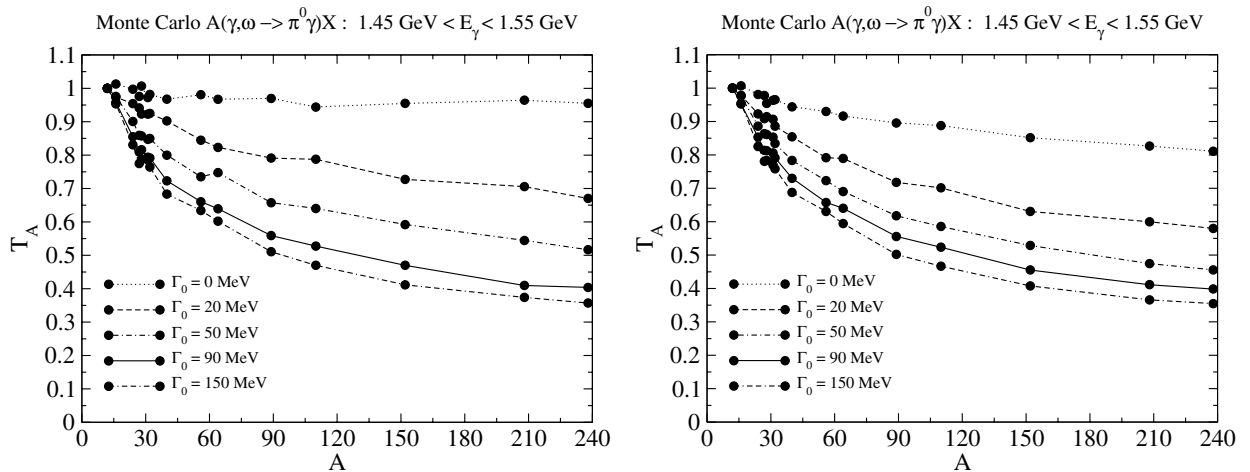
Fig. 2. The result of the Monte Carlo method for the A-dependence of the nuclear transparency ratio T_A without (left panel) and with (right panel) FSI of outgoing pions. A lower cut $T_\pi > 150\,\mathrm{MeV}$ on the kinetic energy of the outgoing pions has been used to suppress the contribution of the distorted events due to FSI. The incident photon beam was constrained in the range $1.45\,\mathrm{GeV} < E_\gamma < 1.55\,\mathrm{GeV}$. The carbon $^{12}\mathrm{C}$ was used as the reference target in the ratio of the nuclear cross-sections. With $\Gamma_{abs} = \Gamma_0 \frac{\rho(r)}{\rho_0}$, where ρ_0 is the normal nuclear-matter density, the dotted, dashed, dash-dotted, solid and double-dash–dotted curves correspond to $\Gamma_0 = 0\,\mathrm{MeV}$, $\Gamma_0 = 20\,\mathrm{MeV}$, $\Gamma_0 = 50\,\mathrm{MeV}$, $\Gamma_0 = 90\,\mathrm{MeV}$ and $\Gamma_0 = 150\,\mathrm{MeV}$, respectively.

And using similar isospin arguments the total reaction cross-section may be written in the form

$$\bar{\sigma}_R \equiv \frac{1}{2}(\sigma_{\pi^0 p \to X} + \sigma_{\pi^0 n \to X})$$
$$= \frac{1}{2}(\sigma_{\pi^- p \to X} + \sigma_{\pi^+ p \to X}). \qquad (19)$$

The corresponding probabilities are calculated using the expression similar to eq. (16). The reaction mechanisms corresponding to eqs. (18) and (19) remove the pions from initial flux. Finally, following the steps and parameterizations of ref. [33] we get the extrapolation of the two- and three-body absorption mechanisms to higher kinetic energies of the pions.

5 In-medium ω-meson width and nuclear transparency

In this section we discuss an extraction of the in-medium inelastic width of the ω in the photonuclear experiments. As a measure for the ω-meson width in nuclei we employ the so-called nuclear transparency ratio

$$\tilde{T}_A = \frac{\sigma_{\gamma A \to \omega X}}{A \sigma_{\gamma N \to \omega X}}, \qquad (20)$$

i.e. the ratio of the nuclear ω-photoproduction cross-section divided by A times the same quantity on a free nucleon. $\tilde{T}_A$ describes the loss of flux of ω-mesons in the nuclei and is related to the absorptive part of the ω-nucleus optical potential and thus to the ω width in the nuclear medium. Furthermore, the A-dependence of the nuclear transparency ratio should reflect the modification of the ω-meson width with increasing nuclear-matter density. This method has been already proven to be very efficient in the study of the in-medium properties of the

vector mesons [36–38] and hyperons [39]. In ref. [21] the transparency ratio has been already used to determine the width of the ω-meson in finite nuclei using the BUU transport approach.

We have done the MC calculations for the sample nuclear targets: $^{12}_6\mathrm{C}$, $^{16}_8\mathrm{O}$, $^{24}_{12}\mathrm{Mg}$, $^{27}_{13}\mathrm{Al}$, $^{28}_{14}\mathrm{Si}$, $^{31}_{15}\mathrm{P}$, $^{32}_{16}\mathrm{S}$, $^{40}_{20}\mathrm{Ca}$, $^{56}_{26}\mathrm{Fe}$, $^{64}_{29}\mathrm{Cu}$, $^{89}_{39}\mathrm{Y}$, $^{110}_{48}\mathrm{Cd}$, $^{152}_{62}\mathrm{Sm}$, $^{208}_{82}\mathrm{Pb}$, $^{238}_{92}\mathrm{U}$. In the following we evaluate the ratio between the nuclear cross-sections in heavy nuclei and a light one, for instance $^{12}\mathrm{C}$, since in this way, many other nuclear effects not related to the absorption of the ω cancel in the ratio [37]. We call this ratio T_A.

The results of the MC calculation for the A-dependence of the nuclear transparency ratio T_A are presented in fig. 2. The incident photon beam was constrained in the range $1.45\,\mathrm{GeV} < E_\gamma < 1.55\,\mathrm{GeV}$ —a region which is considered in the analysis of the CBELSA/TAPS experiment [40,41]. The carbon $^{12}\mathrm{C}$ was used as the reference target in the ratio of the nuclear cross-sections. In fig. 2 (left panel) we show the results for the transparency ratio when the collisional broadening and FSI of the ω are taken into account but without FSI of the pions from $\omega \to \pi^0 \gamma$ decays inside the nucleus. With $\Gamma_{abs} = \Gamma_0 \frac{\rho(r)}{\rho_0}$ the dotted, dash-dotted, solid and double-dash–dotted curves in fig. 2 (left panel) correspond to $\Gamma_0 = 0\,\mathrm{MeV}$ (no ω absorption), $\Gamma_0 = 20\,\mathrm{MeV}$, $\Gamma_0 = 50\,\mathrm{MeV}$, $\Gamma_0 = 90\,\mathrm{MeV}$ and $\Gamma_0 = 150\,\mathrm{MeV}$, respectively. In the case without ω-absorption we do not observe any significant decrease of the T_A. Furthermore, assuming that the distortion factor in eq. (1) is $\Omega_\omega = 1$ (no FSI at all) leads essentially to the same result. For other values of the absorption parameter Γ_0 a very strong attenuation of the $\omega \to \pi^0 \gamma$ signal with increasing nuclear-mass number A is noted. This is primary due to the stronger absorption of the ω-mesons with increasing nuclear-matter density, see eq. (15). Also the

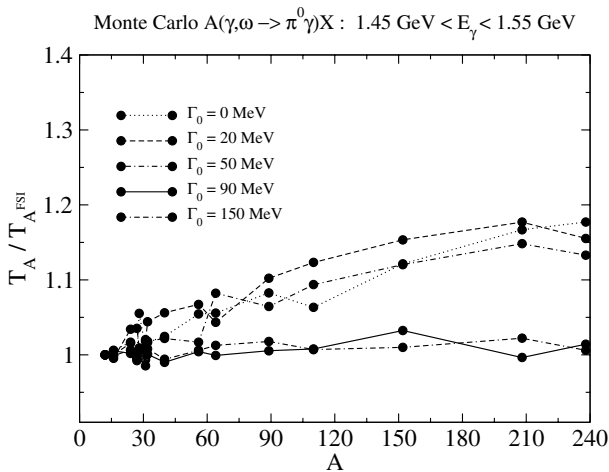Monte Carlo $A(\gamma,\omega \rightarrow \pi^0\gamma)X$: 1.45 GeV < E_γ < 1.55 GeV

Fig. 3. The result of the Monte Carlo method for the A-dependence of the ratio T_A/T_A^{FSI} where T_A is calculated without (left panel of fig. 2) and T_A^{FSI} with (right panel of fig. 2) FSI of outgoing pions. A lower cut $T_\pi > 150\,\mathrm{MeV}$ on the kinetic energy of the outgoing pions has been used to suppress the contribution of the distorted events due to FSI. The incident photon beam was constrained in the range $1.45\,\mathrm{GeV} < E_\gamma < 1.55\,\mathrm{GeV}$. Notations for the curves are the same as in fig. 2.

contribution of the ω-mesons decaying inside the nucleus is increasing as a function of the mass number A merely due to an increase in the effective radius of the nucleus.

We have already noted that the FSI of the pions (π-FSI) distorts the $\pi^0\gamma$ spectra and the reconstructed $\pi^0\gamma$ pairs contain events from the quasielastic steps which basically lose all information about their source. These $\pi^0\gamma$ pairs do not go into the final detection channel since they appear at much smaller invariant masses. It was already demonstrated in refs. [42,19] that the contributions of the distorted events due to the FSI of the pions can be largely suppressed by using a lower cut $T_\pi > 150\,\mathrm{MeV}$ on the kinetic energy of the outgoing pions. A typical π^0 kinetic energy in the process is $T_\pi \simeq 380\,\mathrm{MeV}$, hence removing pions with $T_\pi < 150\,\mathrm{MeV}$ does indeed eliminate the pions which certainly underwent some quasielastic collisions.

We therefore use this cut in the full MC simulation and, next, we consider the situation when both ω and π^0 are subject to FSI in their way out of the nucleus. The results of the MC simulation with the ω/π-FSI and a cut $T_\pi > 150\,\mathrm{MeV}$ are shown in fig. 2 (right panel). As one can see the effect of the π-FSI on T_A is sizable at small values of the absorption parameter Γ_0. Note that a decrease of the ratio T_A at $\Gamma_0 = 0\,\mathrm{MeV}$ is caused both by the stronger π-absorption at higher nuclear-matter densities and because of the cut we have imposed to remove the pions interacting via quasielastic scattering from the total flux. But since the dependence of the transparency ratio on the ω width is non-linear, the impact of the π-FSI is already very small at $\Gamma_0 \simeq 90\,\mathrm{MeV}$. At this value of the ω width the two curves with (right panel) and without (left panel) π-FSI are very close to each other. This can be seen in fig. 3 where we have plotted the ratio T_A/T_A^{FSI} with T_A and T_A^{FSI} calculated without and with FSI of outgoing

pions, respectively. This moderate effect of the FSI of the pions should also apply to the pions of the background from $\pi^0\pi^0$ production or uncorrelated (no ω) $\pi^0\gamma$ events, to which we shall come back in sect. 7.

6 The eikonal (Glauber) approximation

In the following we calculate the nuclear transparency ratio and the distortion factor due to the ω absorption using the eikonal (or Glauber) approximation. In this framework the propagation of the ω in its way out of the nucleus can be accounted for by means of the exponential factor describing the loss of flux probability per unit length. This simple but rather reliable method will allow us to get an accurate result for the integrated cross-sections without performing an elaborate MC simulation.

We proceed as follows: let Π_ω be the ω self-energy in the nuclear medium as a function of the nuclear density, $\rho(r)$. We have for the collisional width

$$\frac{\Gamma_\omega}{2} = -\frac{\mathrm{Im}\,\Pi_\omega}{2E_\omega}, \quad \Gamma_\omega \equiv \frac{\mathrm{d}P}{\mathrm{d}t}, \tag{21}$$

where P is the probability of ω interaction in the nucleus, including ω quasielastic collisions and absorption channels. We shall not consider the part of the $\mathrm{Im}\,\Pi_\omega$ due to the quasielastic collisions since, even if the nucleus gets excited, the ω will still be there to be observed. Thus, mainly the absorption of the ω is reflected in the loss of ω events in the nuclear production as we have already demonstrated using the MC method. This part of the ω self-energy is the one discussed before, see eq. (15). Hence, we have for the loss of flux probability per unit length

$$\frac{\mathrm{d}P}{\mathrm{d}l} = \frac{\mathrm{d}P}{v\,\mathrm{d}t} = \frac{\mathrm{d}P}{\frac{|\vec{p}_\omega|}{E_\omega}\mathrm{d}t} = \frac{E_\omega}{|\vec{p}_\omega|}\Gamma_{abs} \tag{22}$$

and the corresponding survival probability is given by

$$\exp\left[\int_0^\infty \mathrm{d}l(-1)\frac{E_\omega}{|\vec{p}_\omega|}\Gamma_{abs}\Big(\rho(\vec{r}')\Big)\right], \tag{23}$$

where $\vec{r}' = \vec{r} + l\frac{\vec{p}_\omega}{|\vec{p}_\omega|}$ with $\vec{r}$ being the ω production point inside the nucleus.

Then the total photonuclear cross-section $A(\gamma,\omega)X$ is given by eq. (1) where now the kernel Ω_ω is replaced by the eikonal factor of eq. (23). Since, the integration over $\widetilde{m}_\omega^2$ in eq. (1) should not change the normalization of the total cross-section, one can use in eq. (1) the spectral function of the free ω, $S_\omega \rightarrow S_\omega^{free}$.

The results of the eikonal approximation for the A-dependence of the nuclear transparency ratio T_A are shown in fig. 4 (left panel). The kinematic constraints and notations for the curves are the same as in fig. 2. In fig. 4 (right panel) we compare the A-dependence of the nuclear transparency ratio calculated using the Monte Carlo simulation method (solid curve) and the eikonal approximation (dashed curve). In both cases we used the
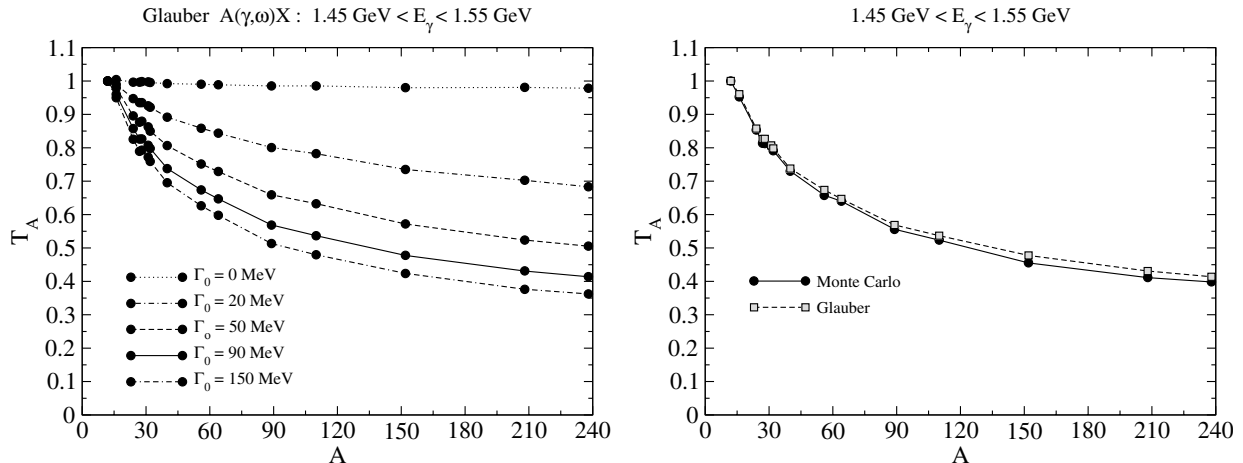
Fig. 4. Left panel: the A-dependence of the nuclear transparency ratio T_A when using the eikonal approximation (see the text). The notations for the curves are the same as in fig. 2. Right panel: comparison of the A-dependence of the nuclear transparency ratio calculated using the Monte Carlo simulation method (solid curve) and the eikonal approximation (dashed curve). The inelastic width of the ω of $\Gamma_0 = 90\,\mathrm{MeV}$ at ρ_0 has been assumed in both calculations.

collisional width (absorptive part) of 90 MeV at normal nuclear-matter densities ρ_0, which gives a fair description of the preliminary data of the CB/TAPS Collaboration [41]. As one can see, the two curves are very close to each other suggesting a remarkable accuracy of the eikonal approximation. See also related discussions in ref. [21].

There are essential differences in the two approaches. In the eikonal approximation the ω proceeds always in the forward direction after any collision following the straight trajectories in their way out of the nucleus. Furthermore, in the eikonal approximation the ω-mesons keep always their original energy, which is not the case in the MC simulation, where because of the quasielastic steps the energy depends on the scattering angle. Also the FSI of the pions coming from the interior of the nucleus is not accounted for in the eikonal formula. In spite of that, the results of both methods are rather similar. Although the eikonal method is very accurate for the total cross-sections at rather big values of the absorption parameter Γ_0, it cannot be used for the detailed studies of the differential spectra where the acceptance conditions relevant for the actual experiment must be taken into account like the MC simulation method does.

The discussion above illustrates why the eikonal approximation works well for the total ω production rate. The quasielastic ω collisions are not taken into account in this approach, but they only produce changes in the ω direction and energy, not in the ω counts. Furthermore, the ω produced, after rescattering, will keep as an average the direction in which it was produced. Finally, using the results of both methods and taking into account the preliminary results of CBELSA/TAPS experiment [41] we get an estimate for the ω width:

$$\Gamma_{abs} \simeq 90 \times \frac{\rho(r)}{\rho_0}\,\mathrm{MeV}. \qquad (24)$$

This estimate must be understood as an average over the ω three-momentum. By this we conclude that the measure-

ments of the A-dependence of the nuclear transparency ratio provide very important information on the absorptive part of the ω-meson width in the nuclear medium.

7 In-medium ω-meson mass and CBELSA/TAPS experiment

As we have already seen in the previous sections the ω-mesons which have an increased decay probability inside the nucleus may carry experimentally observable information concerning their in-medium properties. Furthermore, the ω-mesons decaying inside nuclei can be used for studying their in-medium properties. Success in finding experimental information on these properties suggests to take a certain kinematic condition where the decay length $L_\omega = |\vec{p}_\omega|/m_\omega\Gamma_\omega$ of the ω moving with the three-momentum $|\vec{p}_\omega|$ should be less than the nuclear radius. Therefore, in the actual experiment it is preferred that the kinetic energy of the ω-meson is small, since in this case, the fraction of ω-mesons decaying inside the nucleus can be increased further merely by minimizing the ω decay length. This can be achieved with an incident photon energy close to the ω-production threshold or using the kinematical cuts on the ω-meson three-momentum, as have been demonstrated in refs. [42,19]. The later idea to gate the ω momenta using the higher momentum cuts has been used in a recent CBELSA/TAPS experiment where a significant modification of the ω-meson line shape when these mesons are produced in a dense medium was reported [28]. This change of the $\pi^0\gamma$ invariant-mass spectra and an accumulation of additional strength at lower invariant masses was interpreted as an evidence for the lowering of the ω mass in nuclei.

At the same time one should note, that the ω line shape reconstructed from $\pi^0\gamma$ events strongly depends on the background shape subtracted from the bare $\pi^0\gamma$ signal. In ref. [28] the shape of the background was chosen
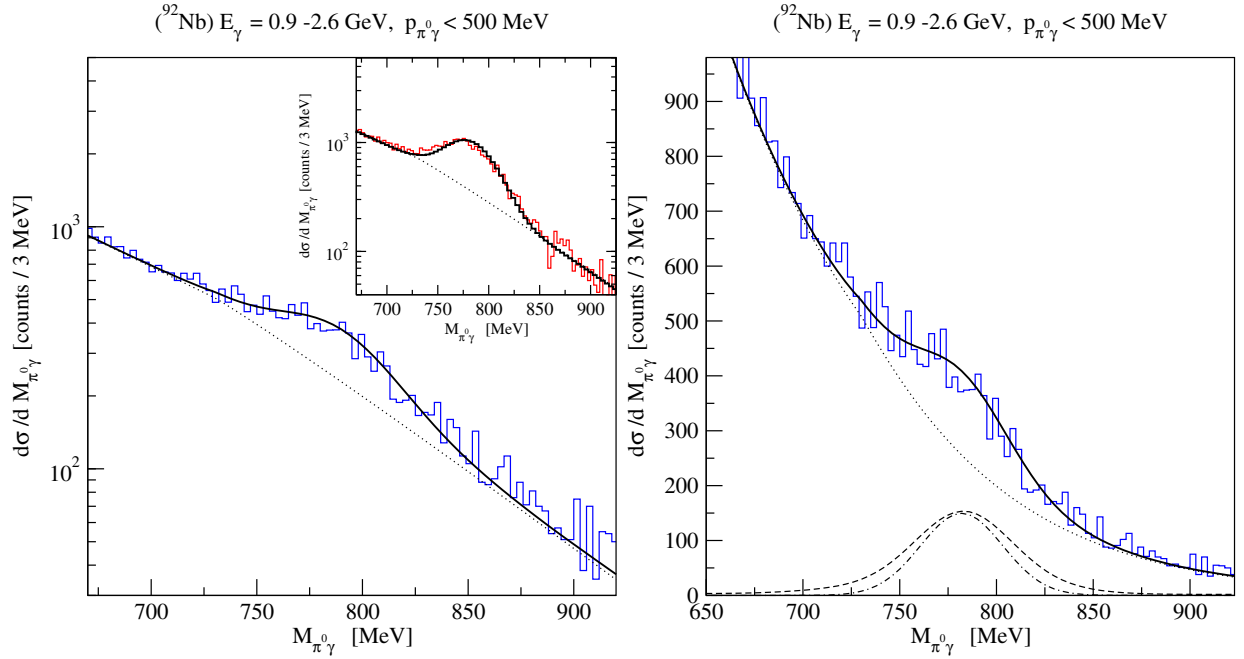
Fig. 5. Left panel: invariant-mass spectra reconstructed from the $\pi^0\gamma$ events in the $(\gamma, \pi^0\gamma)$ reaction from the Nb target (solid curve). The experimental data are from ref. [28]. The incident photon beam has been constrained in the range $0.9\,\text{GeV} < E_\gamma^{in} < 2.6\,\text{GeV}$. The dotted curve is an uncorrelated $\pi^0\gamma$ background (see the text). Right panel: the same as the left panel but in linear scale. The dashed and dash-dotted curves correspond to the $\omega \to \pi^0\gamma$ events with and without the kinematic cut $|\vec{p}_{\pi^0\gamma}| < 500\,\text{MeV}$, respectively. The normalization without cut is arbitrary. The solid line corresponds to the sum of the background and the dashed line. Inset (left panel): the $\pi^0\gamma$ invariant-mass spectra in the elementary $p(\gamma, \pi^0\gamma)p$ reaction. The same background line shape (dotted curve) as for the Nb target has been used. The solid line is the sum of the background and $\omega \to \pi^0\gamma$ events.

such that it accounted for all the experimental strength at large invariant masses. This choice was done both for the elementary $\gamma p \to \pi^0\gamma p$ reaction as well as for nuclei. As we shall show, this choice of background in nuclei implies a change of the shape from the elementary reaction to that in the nucleus for which no justification was given. We shall also show that when the same shape for the background as for the elementary reaction is chosen, the experiment in nuclei shows strength at invariant masses higher than m_ω where the choice of [28] necessarily produced no strength. We will also see that the experimental data can be naturally interpreted in terms of the large in-medium ω width discussed above without the need to invoke a shift in the ω mass in the medium.

In fig. 5 we show the experimental data (solid histogram) for the $\pi^0\gamma$ invariant-mass spectra in the reaction $(\gamma, \pi^0\gamma)$ [28] from the $^{92}_{41}$Nb target. The inset (left panel) corresponds to the $\pi^0\gamma$ spectra from the hydrogen target. In our MC calculations the incident photon beam has been constrained in the range $0.9\,\text{GeV} < E_\gamma^{in} < 2.6\,\text{GeV}$. The higher momentum cut $|\vec{p}_{\pi^0\gamma}| = |\vec{p}_{\pi^0} + \vec{p}_\gamma| < 500\,\text{MeV}$ on a three-momentum of the $\pi^0\gamma$ pair was imposed as in the actual experiment. First, we use the hydrogen target, see inset in fig. 5 (left panel), to fix the contribution of the uncorrelated $\pi^0\gamma$ background (dotted curve) which together with the $\pi^0\gamma$ signal from $\omega \to \pi^0\gamma$ decay, folded with the Gaussian experimental resolution of 55 MeV as

in ref. [28], gives a fair reproduction of the experimental spectra. Then we assume the same shape of the $\pi^0\gamma$ background in the photonuclear reaction. Assuming the same shape does not imply that there is no modification of the background in the nucleus. That is, we do not imply that $\sigma_A = A\sigma_N$ for the background, but only that we can take the same proportionality factor between σ_A and σ_N in a region of 100–150 MeV for $M_{\pi^0\gamma}$ around the ω peak. The weak effect of the FSI of the pions found in sect. 5, with the cuts imposed in the experiment, strongly supports this assumption.

In the following we use the ω inelastic width of $\Gamma_0 = 90\,\text{MeV}$ at ρ_0. The exclusive $\omega \to \pi^0\gamma$ MC spectra is shown by the dashed curve (right panel). The solid curve is the reconstructed $\pi^0\gamma$ signal after applying the cut on $\pi^0\gamma$ momenta and adding the background fixed when using the hydrogen target (dotted curve). Note that the shape of the exclusive $\pi^0\gamma$ signal without applying a cut on $\pi^0\gamma$ momenta (dash-dotted curve) is dominated by the experimental resolution and no broadening of the ω is observed. This is in agreement with the data of ref. [28]. But applying the cut one increases the fraction of in-medium decays coming from the interior of the nucleus where the spectral function is rather broad and as a result the broadening of the $\pi^0\gamma$ signal with respect to the signal (without cut) can be well seen. The resulting MC spectra (solid curve) shows the accumulation of the $\pi^0\gamma$ events from the left
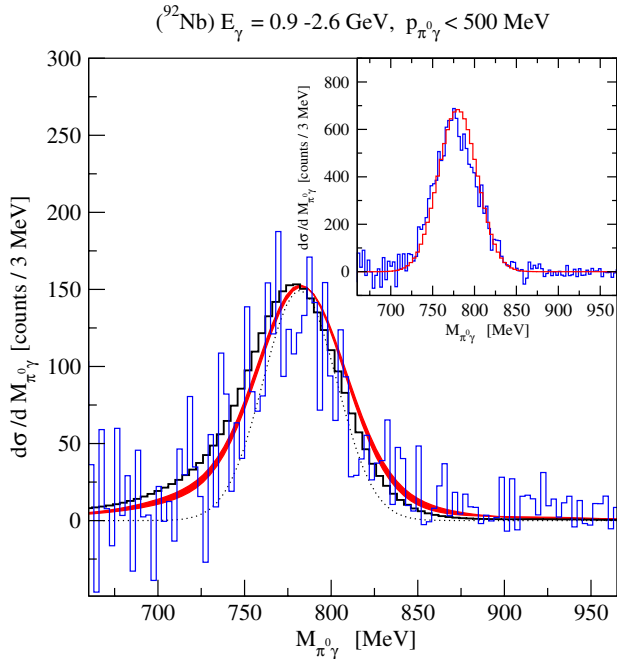
Fig. 6. Invariant-mass spectra reconstructed from $\pi^0\gamma$ events. The kinematic constraints are the same as in fig. 5. The band corresponds to the changes of the in-medium ω mass according to $m_\omega \pm 40(\rho/\rho_0)$ MeV. The serrated line corresponds to the scaling of the ω mass $m_\omega(1 - 0.16\rho/\rho_0)$. The dotted curve is the $\omega \to \pi^0\gamma$ signal without applying the kinematic cuts. The background (dotted curve in fig. 5) has been subtracted from the experimental data of ref. [28]. See the text for further explanations. Inset: the $\pi^0\gamma$ signal from the hydrogen target.

and right sides of the mass spectra, and it is consistent both with our choice of the uncorrelated $\pi^0\gamma$ background and experimental data.

It is interesting to stress here that the choice of the background done in [28] significantly changes it from the proton target to the nucleus. Indeed, inspection of fig. 5 (a) of ref. [28] clearly shows that while the background on the proton has a kind of convex parabolic form (see this also in fig. 5 here, inset), the background chosen for Nb in [28] is a straight line in the logarithmic plot. This increases the assumed background with respect to that induced from the proton experiment at high masses which is difficult to justify. Indeed, even if the distortion on the pions from FSI is not large, its effect should go into degrading the pion energy and consequently moving events to lower $\pi^0\gamma$ invariant masses, hence reducing relatively the background at higher $\pi^0\gamma$ masses, not increasing it.

We have also done the exercise of seeing the sensitivity of the results to changes in the mass. In the dark band of fig. 6 we show the results of having the ω mass in between $m_\omega \pm 40\rho/\rho_0$ MeV. The narrowness of the band indicates that the experimental data could not be precise enough to distinguish between these cases. In other words, this experiment is too insensitive to changes in the mass to be used for a precise determination of the shift of the ω mass in the nuclear medium. On the other hand, we have shown that the results are more sensitive to changes in

the width of the ω in the medium. This is due to the fact that an increased width produces more decays of the ω in the medium which allows one to see changes in the $\pi^0\gamma$ spectra. This larger sensitivity of the results to the width than to mass change was already observed in studies of the ρ production in nuclei [43]. In any case, we have checked what the results would be should we assume $m_\omega(1 - 0.16\rho/\rho_0)$, *i.e.*, a shift of 125 MeV at $\rho = \rho_0$ as suggested in ref. [3]. We can see the results in the thick serrated line in fig. 6 which shows a visible asymmetry with respect to the dark band, the one we have shown to be compatible with experiment for our choice of background. We should note that the peak position barely moves since it is dominated by the decay of the ω outside the nucleus.

8 Conclusions

We have performed calculations of the $(\gamma A \to \pi^0\gamma X)$ reaction for $\pi^0\gamma$ invariant masses around the ω mass. A clear signal is seen in the experiment for ω production with subsequent $\pi^0\gamma$ decay, both for the elementary reaction on a proton target as well as in the nuclear targets. In addition there is a sizable background that has to be subtracted in order to identify the ω signal in the proton and nuclear targets. We have performed a Monte Carlo simulation of the ω production followed by its decay into $\pi^0\gamma$, with a detailed study of the final-state interaction of the particles involved in the process. The invariant mass distribution of the $\pi^0\gamma$ pairs is evaluated when the particles have left the nucleus. We compare our theoretical results with the experimental data and induce from there that the data are compatible with an ω in the medium width of around 90 MeV at normal nuclear matter and no shift in the mass. This large width in the medium is compatible with preliminary results obtained from the transparency ratio in ω production in nuclei for which we also present theoretical results here.

The results obtained here for the mass shift disagree with those formerly claimed in [28] and we show that the reason for this discrepancy is due to a different choice of background. In [28] the background for nuclear targets did not scale with respect to the one on proton targets and the shape assumed for both targets was manifestly different. The choice of background in nuclei was done such as to cut the contribution of high ω invariant masses. By means of this choice, the shape of the ω mass distribution in nuclei was asymmetric, showing additional strength only at masses smaller than the ω mass which induced the authors to claim that there was a shift of mass to lower invariant masses. We have done a different choice of background, more suited for the studied reaction, which is to take the same shape for the background in nuclei as for the proton target. With this choice of background, the ω invariant-mass distribution is symmetric and explained in terms of the enlarged ω width in the medium with no need to invoke a shift in the mass. We also show that the reaction is not well suited to make precise determinations of the mass, and see that the data could not distinguish between masses in a range $m_\omega \pm 40\rho/\rho_0$ MeV.

References

1. M. Post, S. Leupold, U. Mosel, Nucl. Phys. A **741**, 81 (2004) [arXiv:nucl-th/0309085].
2. G.E. Brown, M. Rho, Phys. Rev. Lett. **66**, 2720 (1991).
3. T. Hatsuda, S.H. Lee, Phys. Rev. C **46**, 34 (1992).
4. V. Bernard, Ulf-G. Meissner, Nucl. Phys. A **489**, 647 (1988).
5. H.C. Jean, J. Piekarewicz, A.G. Williams, Phys. Rev. C **49**, 1981 (1994).
6. F. Klingl, N. Kaiser, W. Weise, Nucl. Phys. A **624**, 527 (1997).
7. K. Saito, K. Tsushima, A.W. Thomas, A.G. Williams, Phys. Lett. B **433**, 243 (1998).
8. K. Tsushima, D.H. Lu, A.W. Thomas, K. Saito, Phys. Lett. B **443**, 26 (1998).
9. B. Friman, Acta Phys. Pol. B **29**, 3195 (1998).
10. F. Klingl, T. Waas, W. Weise, Nucl. Phys. A **650**, 299 (1999).
11. M. Post, U. Mosel, Nucl. Phys. A **688**, 808 (2001).
12. K. Saito, K. Tsushima, D.H. Lu, A.W. Thomas, Phys. Rev. C **59**, 1203 (1999).
13. G.I. Lykasov, W. Cassing, A. Sibirtsev, M.V. Rzyanin, Eur. Phys. J. A **6**, 71 (1999).
14. A. Sibirtsev, C. Elster, J. Speth, arXiv:nucl-th/0203044.
15. A.K. Dutt-Mazumder, R. Hofmann, M. Pospelov, Phys. Rev. C **63**, 015204 (2001).
16. M.F.M. Lutz, G. Wolf, B. Friman, Nucl. Phys. A **706**, 431 (2002); **765**, 431 (2006)(E).
17. S. Zschocke, O.P. Pavlenko, B. Kampfer, Phys. Lett. B **562**, 57 (2003) [arXiv:hep-ph/0212201].
18. A.K. Dutt-Mazumder, Nucl. Phys. A **713**, 119 (2003).
19. P. Muhlich, T. Falter, U. Mosel, Eur. Phys. J. A **20**, 499 (2004) [arXiv:nucl-th/0310067].
20. P. Muehlich, V. Shklyar, S. Leupold, U. Mosel, M. Post, arXiv:nucl-th/0607061.
21. P. Muhlich, U. Mosel, Nucl. Phys. A **773**, 156 (2006).
22. B. Steinmueller, S. Leupold, arXiv:hep-ph/0604054.
23. U. Mosel, Prog. Part. Nucl. Phys. **42**, 163 (1999).
24. E325 Collaboration (K. Ozawa *et al.*), Phys. Rev. Lett. **86**, 5019 (2001) [arXiv:nucl-ex/0011013].
25. T. Tabaru *et al.*, Phys. Rev. C **74**, 025201 (2006).
26. E325 Collaboration (F. Sakuma *et al.*), arXiv:nucl-ex/0606029.
27. D. Weygand, talk at the *QNP06 Conference, Madrid, June 2006*; C. Djalali, talk at the *YKIS06 Workshop, Kyoto, December 2006*.
28. CBELSA/TAPS Collaboration (D. Trnka *et al.*), Phys. Rev. Lett. **94**, 192303 (2005) [arXiv:nucl-ex/0504010].
29. J. Barth *et al.*, Eur. Phys. J. A **18**, 117 (2003).
30. W.-M. Yao *et al.*, J. Phys. G **33**, 1 (2006).
31. L.L. Salcedo, E. Oset, M.J. Vicente-Vacas, C. Garcia-Recio, Nucl. Phys. A **484**, 557 (1988).
32. E. Oset, L.L. Salcedo, D. Strottman, Phys. Lett. B **165**, 13 (1985).
33. E. Oset, D. Strottman, Phys. Rev. C **42**, 2454 (1990).
34. E. Hernandez, E. Oset, Nucl. Phys. A **455**, 584 (1986).
35. The CNS Data Analysis Center, `http://gwdac.phys.gwu.edu`.
36. T. Ishikawa *et al.*, Phys. Lett. B **608**, 215 (2005).
37. V.K. Magas, L. Roca, E. Oset, Phys. Rev. C **71**, 065202 (2005).
38. P. Muhlich, U. Mosel, Nucl. Phys. A **765**, 188 (2006).
39. M. Kaskulov, L. Roca, E. Oset, Eur. Phys. J. A **28**, 139 (2006) [arXiv:nucl-th/0601074]; M. Kaskulov, E. Oset, Phys. Rev. C **73**, 045213 (2006) [arXiv:nucl-th/0509088].
40. D. Trnka, PhD Thesis, University of Giessen, 2006.
41. M. Kotulla, arXiv:nucl-ex/0609012.
42. J.G. Messchendorp, A. Sibirtsev, W. Cassing, V. Metag, S. Schadmand, Eur. Phys. J. A **11**, 95 (2001).
43. E. Oset, L. Roca, M.J. Vicente Vacas, J.C. Nacher, *International Workshop on Chiral Fluctuations in Hadronic Matter, Orsay, September 2001*, arXiv:nucl-th/0112033.